

One-nucleon transfer reactions to continuum states induced by heavy ion projectiles

I. Lhenry,¹ T. Suomijärvi,¹ Y. Blumenfeld,¹ Ph. Chomaz,² N. Francaria,¹ J. P. Garron,¹

J. C. Roynette,¹ J. A. Scarpaci,¹ D. Beaumel,¹ S. Fortier,¹ S. Gales,¹

H. Laurent,¹ A. Gillibert,³ G. M. Crawley,⁴ J. Finck,⁵ G. Yoo,⁴ and J. Barreto^{1,6}

¹*Institut de Physique Nucléaire, IN2P3-CNRS, 91406 Orsay, France*

²*GANIL, BP 5027, 14021 Caen, France*

³*SPhN-DAPNIA, CE Saclay, 91191 Gif-sur-Yvette, France*

⁴*NSCL MSU, East Lansing, Michigan 48824*

⁵*Department of Physics, Central Michigan University, Mt. Pleasant, Michigan 48859*

⁶*Universidade Federal, Rio de Janeiro 21945, Brazil*

(Received 7 March 1995; revised manuscript received 12 April 1996)

High-lying excitations were studied by means of the $^{207}\text{Pb} \rightarrow ^{208}\text{Pb}$, $^{209}\text{Bi} \rightarrow ^{210}\text{Bi}$, and $^{59}\text{Co} \rightarrow ^{60}\text{Ni}$ stripping reactions and $^{209}\text{Bi} \rightarrow ^{208}\text{Pb}$ and $^{63}\text{Cu} \rightarrow ^{62}\text{Ni}$ pickup reactions induced by ^{20}Ne and ^{36}Ar projectiles at 48 and 42 MeV/nucleon, respectively. In the stripping spectra, structures a few MeV wide are observed at excitation energies of 10–15 MeV, embedded in a large continuum. The corresponding Q values suggest that these structures are predominantly due to single-particle excitations rather than to the excitation of collective states such as giant resonances. This interpretation is in agreement with a microscopic calculation showing that in the one-nucleon transfer reactions only a small part of the cross section is due to the collective excitations. The overall shape of the neutron stripping spectra is well reproduced by the semiclassical reaction model of Bonaccorso and Brink, which treats on the same footing both the breakup of the projectile and the transfer to single-particle resonances. [S0556-2813(96)05308-3]

PACS number(s): 25.70.Hi, 24.30.Cz, 25.70.Ef

I. INTRODUCTION

In one-nucleon stripping reactions on ^{90}Zr and ^{208}Pb targets, structures a few MeV wide have been observed at excitation energies of about 15 and 11 MeV, respectively [1–3]. These giant-resonance-like structures are superimposed on a much broader continuum which is commonly interpreted as originating from fast processes, namely, the breakup of the projectile. References [2,3] suggest that these structures are due to the excitation of high-spin single-particle states. The width of these structures (a few MeV) is explained by the coupling of these states to one- and two-photon collective states. Moreover, in a recent experiment, one-nucleon stripping reactions were studied by comparing spectra taken with neighboring target nuclei such as ^{89}Y , ^{90}Zr , and ^{91}Zr , and ^{207}Pb , ^{208}Pb , and ^{209}Bi [4]. In all these spectra, resonancelike structures were also observed. These structures were located at the same Q value for different neighboring targets, while they were shifted in excitation energy which suggested that they were due to the excitation of single-particle states.

However, the bumps observed in several transfer reactions studied with target nuclei in the region of Zr and Pb have excitation energies and widths comparable to those of giant resonances in these nuclei. Therefore, it is a distinct possibility that at least part of the strength observed in these structures could be due to the excitation of such collective states.

It would be interesting to study collective excitations in transfer reactions since nucleon transfer on a target nucleus can be considered as the inverse of the nucleon decay of collective states such as giant resonances to the ground state of the $A-1$ nucleus. Therefore, one could study the micro-

scopic structure of giant resonances and control the different branching ratios extracted from decay studies. Furthermore, one may also hope that transfer reactions would be a good tool to selectively excite different multipole resonances by matching a certain angular momentum through the choice of an appropriate target and projectile combination and bombarding energy. The excitation of collective low-lying 2^+ and 3^- states has already been reported in several one-nucleon stripping reactions with light projectiles [5,6]. To excite the giant resonance region in the spectrum, one needs to bring more energy into the system and thus heavy projectiles are well suited for these studies.

In order to get more insight into collective effects in one-nucleon transfer processes the following reactions were studied, $^{207}\text{Pb} \rightarrow ^{208}\text{Pb}$, $^{209}\text{Bi} \rightarrow ^{210}\text{Bi}$, $^{59}\text{Co} \rightarrow ^{60}\text{Ni}$, $^{209}\text{Bi} \rightarrow ^{208}\text{Pb}$, and $^{63}\text{Cu} \rightarrow ^{62}\text{Ni}$, by using ^{20}Ne projectiles at 48 MeV/nucleon and ^{36}Ar projectiles at 42 MeV/nucleon provided by the accelerator complex at the GANIL national facility, Caen, France. Targets with either one nucleon or one hole outside a closed shell nucleus were chosen in order to produce a closed shell nucleus by adding or removing one nucleon. In these cases, the transfer reactions lead to particle-hole excitations in the closed shell final nucleus. The experimental method and experimental results will be discussed in Secs. II and III, respectively.

To examine theoretically the possibility of exciting collective modes in transfer reactions, we have performed microscopic calculations for one-nucleon stripping reactions on one-hole target nuclei. These are considered as one-step processes where a particle is added to the core and then recoupled via the residual interaction to the normal modes of the target. In these calculations collective states are described within the random phase approximation (RPA) and the col-

lectivity is defined according to the number of configurations, allowed by the transfer reaction, which contribute to a given state. The particle transfer is treated within the distorted-wave Born approximation (DWBA). The results of these microscopic calculations are discussed in Sec. IV.

In the case of stripping reactions, the energy spectrum is dominated by a large bell-shaped continuum. The general assumption about this background has been that it arises from the breakup of the projectile leading to continuum states but no direct confirmation of this assumption in the case of heavy ion reactions is yet available.

To explain the overall shape of the inclusive stripping spectra, Bonaccorso and Brink (BB) have proposed a model [7,8] which gives a description of the neutron transfer reaction to the quasibound and unbound resonant target states as well as an estimation of the contribution of the projectile breakup. Experimental stripping spectra are compared to those calculated by using the Bonaccorso-Brink model and the relative importance of the two components in the inclusive spectra (transfer to resonant states and breakup) will be discussed in Sec. V.

II. EXPERIMENTAL METHOD

Transfer reactions induced by ^{20}Ne and ^{36}Ar beams at 48 and 42 MeV/nucleon, respectively, delivered by the GANIL facility, were performed on the following self-supporting targets: ^{207}Pb (1 mg/cm²), ^{209}Bi (0.8 mg/cm²), ^{59}Co (1.05 mg/cm²), and ^{63}Cu (1.07 mg/cm²). The scattered fragments were analyzed by the energy loss magnetic spectrometer SPEG [9]. For the present experiment two position-sensitive drift chambers were used for the trajectory reconstruction which yielded the focal-plane position and scattering angle of each event.

The identification of fragments was achieved by the simultaneous measurement of their energy loss in an ionization chamber and their time-of-flight between the target and a plastic scintillator located behind the ionization chamber. The start signal for the time-of-flight measurement was provided by the rf of the cyclotron. This detection system allowed an unambiguous mass and charge identification of the scattered fragments.

In order to limit the counting rate, elastically scattered projectiles were stopped by a sliding shield placed in front of the first drift chamber. To measure elastic scattering which was used to obtain absolute normalizations as well as to check energy and angular calibrations, several runs were performed without the shield with a reduced beam intensity.

The spectrometer was set close to the grazing angles for each reaction, i.e., 3° for the Co target and 6° for the Pb and Bi targets. In the last case, an additional run was performed by setting the spectrometer at 3°. The horizontal opening angle of the spectrometer was 4°. The vertical acceptance was limited to about 0.2°. The momentum acceptance of the spectrometer is about 7%, which allowed us to measure several transfer channels as well as the inelastic channel simultaneously.

The overall energy resolution was about 500 keV in the case of neon projectiles and about 800 keV in the case of argon projectiles. The angular resolution was better than 0.2°.

III. EXPERIMENTAL RESULTS

A. One-neutron stripping reactions in the Pb mass region

Figure 1(a) shows the (^{20}Ne , ^{19}Ne) reaction spectra measured for the ^{207}Pb , ^{208}Pb , and ^{209}Bi targets. The three spectra are dominated by a large continuum. The contribution of the breakup of ^{20}Ne to this continuum will be discussed in Sec. V.

In the ^{209}Pb final nucleus, the first low-lying states correspond to neutron transfer to the $2g_{9/2}$ (ground state), $1i_{11/2}$ ($E^*=0.78$ MeV), $1j_{15/2}$ ($E^*=1.43$ MeV), and $2g_{7/2}$ ($E^*=2.49$ MeV) orbitals above the closed $N=126$ core. Excitation energies are from Refs. [2,10,11]. In the present experiment the $1i_{11/2}$ state could not be resolved from the $1j_{15/2}$ state.

As expected from previous studies [2,10,12–14], in high energy transfer reactions, the population of states is mainly governed by the angular momentum selectivity and the initial configuration of the transferred nucleon. In the case of the ^{20}Ne projectiles, the outmost neutron orbitals are $2s_{1/2}$, $1p_{1/2}$, and $1d_{5/2}$ and the neutron transfer is supposed to take place preferentially from these orbitals. Thus the transfer to the first three excited states of ^{19}Ne gives a contribution to the strength measured. The energy difference of these states (less than 0.2 MeV [15]) is much smaller than the experimental energy resolution; therefore, no splitting due to the final state of projectile can be experimentally observed. In order to compare our experimental data with theory, it is necessary to consider the contribution of the three mentioned final states $2s_{1/2}$, $1p_{1/2}$, and $1d_{5/2}$ of ^{19}Ne with respective weights C^2S given by the spectroscopic factors 0.56, 1.97, and 1.03, respectively [15]. The selection rules are included in the calculation of the transfer cross sections with an exact finite-range distorted-wave Born approximation (EFR DWBA) and were found to give generally a good account of the population of low-lying levels observed in the experimental spectra [2,10,11], namely, the dominance of the $1j_{15/2}$ state over the $2g_{9/2}$, $1i_{11/2}$, and $2g_{7/2}$ levels.

In the case of the ^{208}Pb final nucleus, the ground state is formed when a neutron is transferred to the $3p_{1/2}$ hole state in ^{207}Pb . This transition is very weak due to the angular momentum mismatch and is not observed in the spectrum. Because of the coupling of single-neutron states to the hole state of ^{207}Pb , the first excited states $2g_{9/2}$, $1i_{11/2}$, $1j_{15/2}$, and $2g_{7/2}$ in the ^{208}Pb final nucleus are about 3 MeV higher than in ^{209}Pb . The relative population of these low-lying states is very similar to that observed for ^{209}Pb .

The ^{209}Bi target nucleus has a $1h_{9/2}$ proton outside the closed $Z=82$ core. In the ^{210}Bi final nucleus, this proton is coupled to the neutron states in ^{210}Bi . However, this does not significantly modify their excitation energies and the states corresponding to the transfer to $2g_{9/2}$, $1i_{11/2}$, $1j_{15/2}$, and $2g_{7/2}$ neutron orbitals are observed at very similar excitation energies as the corresponding single neutron states in ^{209}Pb and with the same relative yield.

At higher excitation energies, a pronounced bump can be seen in all spectra. In the case of ^{208}Pb , it is located at about 13.5 MeV while in the case of ^{209}Pb and ^{210}Bi it is at about 10 MeV excitation energy. These structures are superimposed on a large continuum partly due to transfer to unbound target states and also probably to projectile breakup pro-

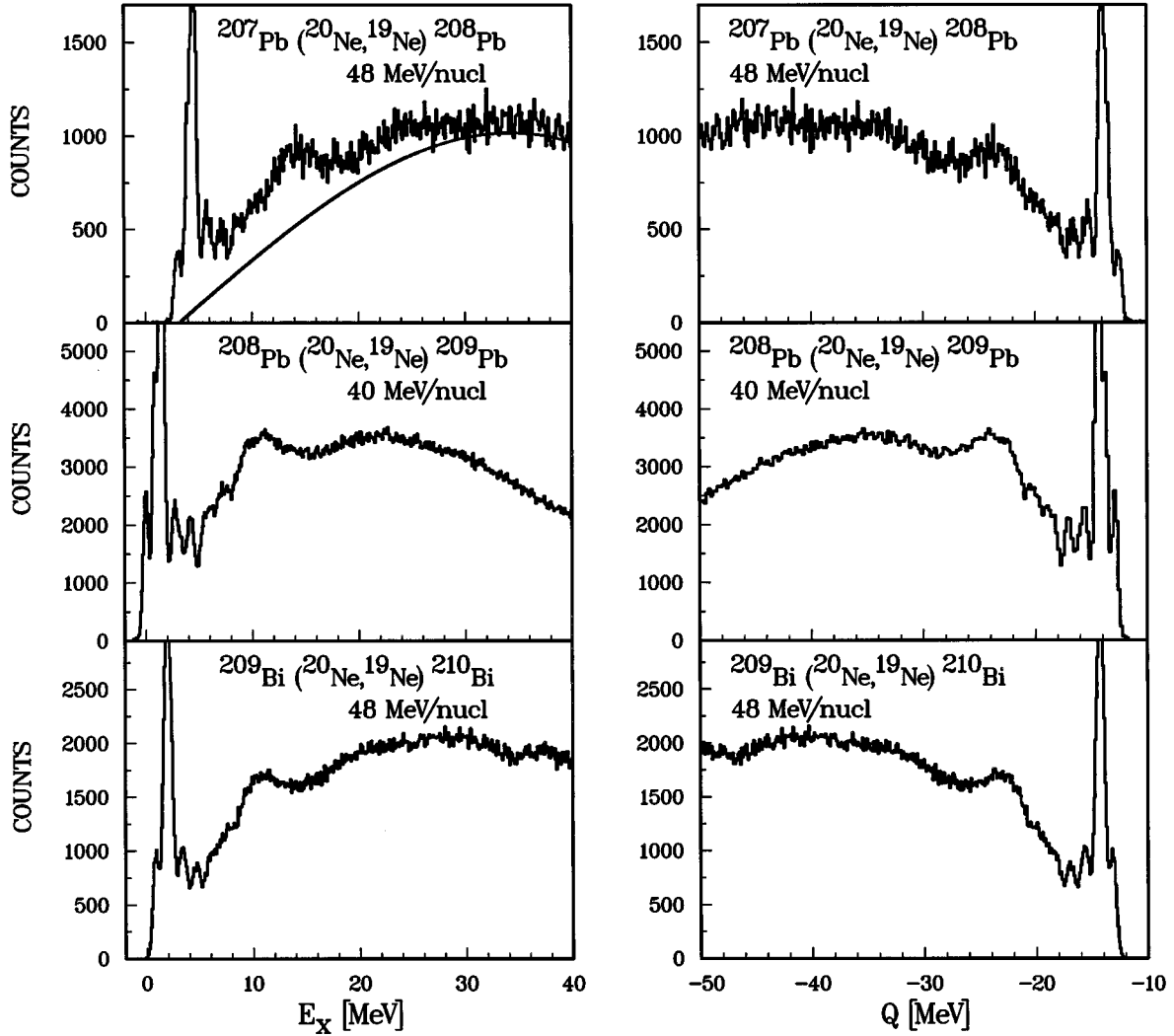


FIG. 1. (a) Energy spectra measured for ^{207}Pb , ^{208}Pb , and ^{209}Bi target nuclei in ($^{20}\text{Ne}, ^{19}\text{Ne}$) stripping reactions. The spectrum for ^{208}Pb target is from Ref. [1]. (b) Same spectra plotted as a function of the Q value.

cesses. Figure 1(b) displays the same spectra in a Q -value scale calculated by $Q = Q_{\text{g.s.}} - E^*$. The previously discussed low-lying states are located at the same Q value for all three reactions. Moreover, the Q value of the structure at high excitation energy is about -23 MeV for all three reactions. These observations suggest that the structure is due to the neutron transfer to the same orbital in different target nuclei. Furthermore, the excitation energy of giant resonances is a smooth function of nuclear mass and depends only weakly on the nuclear structure. Thus only very small variations are expected for the neighboring nuclei, in contradiction with the observations of Fig. 1(a). Similar results were reported for the same target nuclei in the ($^7\text{Li}, ^6\text{Li}$) reaction at 30 MeV/nucleon [4].

In the case of the $^{207}\text{Pb}(^{20}\text{Ne}, ^{19}\text{Ne})^{208}\text{Pb}$ reaction, an attempt was made to extract a spin and parity assignment for the structure at 13.5 MeV. An arbitrary, smooth background was subtracted from the bidimensional ($E^*, \theta_{\text{c.m.}}$) spectrum. This background, integrated over $\theta_{\text{c.m.}}$, is shown as a solid line in Fig. 1. The peak at 13.5 MeV was then fitted by a Gaussian function at different angles. The angular distribu-

tion obtained is shown in Fig. 2. The experimental angular distribution was fitted by a set of theoretical angular distributions calculated by the DWBA code PTOLEMY [16]. The transfers to the three final states of the ^{19}Ne ejectile cited above were considered with their respective spectroscopic factors. The optical model parameters for the Woods-Saxon potential were obtained from the elastic scattering angular distribution of ^{20}Ne on ^{207}Pb at 48 MeV/nucleon measured during the experiment: $V = 63.3$ MeV, $r_r = 1.1$ fm, and $a_r = 0.637$ fm and $W = 62.4$ MeV, $r_i = 1.1$ fm, and $a_i = 0.637$ fm for the real and imaginary parts, respectively. The code was adapted to calculate transfer to quasibound states by using wave functions obtained from the RPA calculation for ^{208}Pb [17]. The result of the fit is indicated by a solid line in Fig. 2. The experimental angular distribution is well reproduced by a linear combination of angular distributions calculated for neutron transfers to $1k_{17/2}$, $2i_{13/2}$, and $1j_{13/2}$ orbitals with relative weights of 1.8, 0.9, and 0.6, respectively. However, in the present analysis, an important uncertainty arises from the arbitrary background subtraction. Therefore, any firm conclusions about the spin and parity

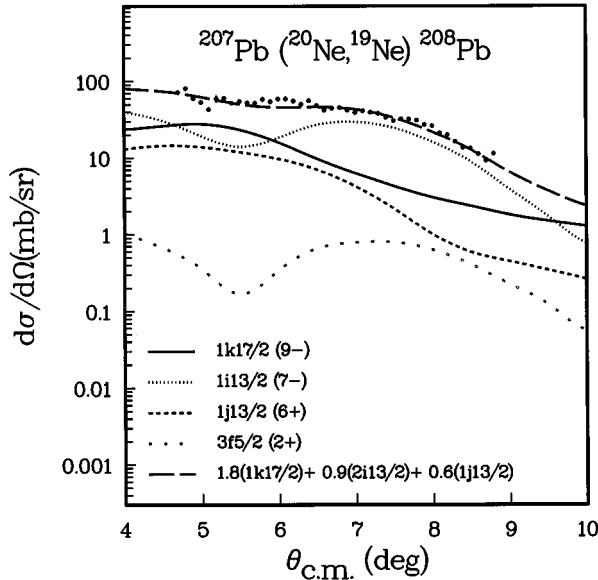


FIG. 2. Angular distribution extracted for the structure observed at 13.5 MeV in the spectrum of $^{207}\text{Pb}(^{20}\text{Ne}, ^{19}\text{Ne})^{208}\text{Pb}$ reaction. Solid line is the result of a fit with theoretical angular distributions for transfer to various neutron orbitals calculated by the DWBA code PTOLEMY.

assignment of the observed structure would require a more precise determination of the background. This can be done by coincident experiments where measuring decay particles at backward angles in coincidence with ejectiles allows the elimination of the projectile breakup contribution from the spectra as shown by Beaumel *et al.* in their recent study of the $^{208}\text{Pb}(\alpha, ^3\text{He})n$ reaction [18].

Figure 3 shows the one-neutron stripping spectrum measured for the ^{207}Pb target with an ^{36}Ar beam at 42 MeV/nucleon. The widths of the first excited states measured with ^{36}Ar projectiles are larger than with the ^{20}Ne beam [Fig. 1(a)], even if the poorer energy resolution is taken into account. At high excitation energies, only a small shoulder can be seen at about 13 MeV while in the case of the ^{20}Ne beam a pronounced bump was observed. This can be partly ex-

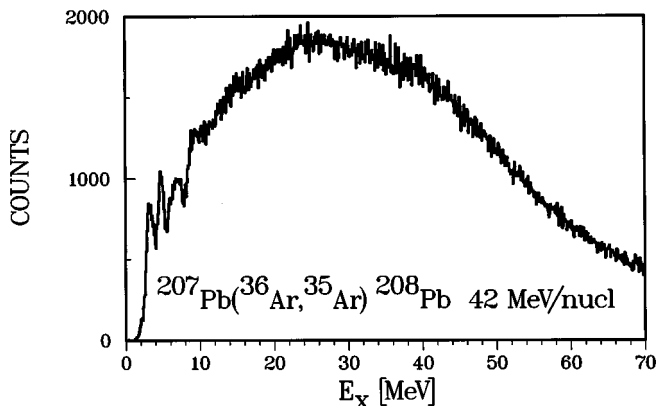


FIG. 3. Energy spectrum measured for the ^{207}Pb target nucleus in the $(^{36}\text{Ar}, ^{35}\text{Ar})$ neutron stripping reaction.

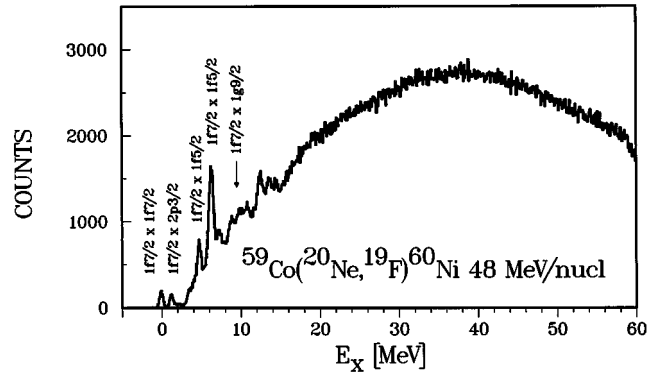


FIG. 4. Energy spectrum measured for the ^{59}Co target nucleus in the $(^{20}\text{Ne}, ^{19}\text{F})$ proton stripping reaction.

plained by the fact that the $^{207}\text{Pb}(^{36}\text{Ar}, ^{35}\text{Ar})^{208}\text{Pb}$ reaction at 42 MeV/nucleon has a smaller matched angular momentum than the same reaction induced by a ^{20}Ne beam at 40 MeV/nucleon and 48 MeV/nucleon. The weak excitation of the $[3p_{1/2}^{-1}1j_{15/2}]$ state of ^{208}Pb (at 4.6 MeV) with the ^{36}Ar beam shows very well the matching difference between the two projectiles. The final states of projectiles need also to be taken into account. In the case of the ^{20}Ne projectile, the energy difference of the first excited states of ejectile was smaller than the experimental resolution; thus, neither a splitting of the low energy states nor a deterioration of resolution could be observed. In the case of the ^{36}Ar projectile, the neutron transfer occurs preferentially from $1d_{3/2}$ and $2s_{1/2}$ orbitals, $1d_{3/2}$ corresponding to the ground state in ^{35}Ar and $2s_{1/2}$ to the first excited state (1.184 MeV). The respective spectroscopic factors for these states are 2.92 and 2.5 [19]. The energy difference of the two possible final states of ^{35}Ar is large and can contribute to the increased width of the peaks in the spectrum. Moreover, the background due to the projectile breakup processes is expected to be very different for ^{36}Ar and ^{20}Ne projectiles, as will be discussed in Sec. V, and the breakup contribution may smear out the high energy structure in the case of ^{36}Ar projectiles.

B. One-proton stripping reaction on ^{59}Co

Figure 4 presents a spectrum measured for the proton stripping reaction $^{59}\text{Co}(^{20}\text{Ne}, ^{19}\text{F})^{60}\text{Ni}$ at 48 MeV/nucleon. As for the ^{19}Ne case, the contribution of the first excited states of the ^{19}F ejectile cannot be resolved in this experiment. The transfer to the $1p_{1/2}$ state of ^{19}F at 0.110 MeV gives the dominant contribution to the spectrum, imposing a strong $j_<$ selectivity.

The target nucleus ^{59}Co has a $1f_{7/2}$ hole in the $N=28$ proton core while neutron shells are filled up to the $2p_{3/2}$ shell. The ground state of ^{60}Ni , which is formed by filling the proton hole, is weakly excited in the studied reaction. The first proton orbitals above the $N=28$ core are $2p_{3/2}$, $2p_{1/2}$, and $1f_{5/2}$. At about 1.3 MeV a small peak corresponding to the $[p_{3/2}, f_{7/2}^{-1}]$ excitation is observed. Because of the dominant $j_<$ selectivity of the projectile and the preferential to high angular momenta, the $[f_{5/2}, f_{7/2}^{-1}]$ state is

strongly excited and the two $T_<$ and $T_>$ components accessed in the present reaction can be clearly seen in the experimental spectrum at 4.7 and 6.2 MeV, respectively. The $[g_{9/2}, f_{7/2}^{-1}]$ state does not benefit from the dominant $j_<$ selectivity of the projectile; thus, it is less excited than the $g_{9/2}$ state in the similar reaction $^{58}\text{Ni}(^{13}\text{C}, ^{12}\text{B})^{59}\text{Cu}$ at 50 MeV/nucleon [20]. The $T_<$ component is located around 6 MeV excitation energy and is mixed with the $T_>$ component of the $[f_{5/2}, f_{7/2}^{-1}]$ state. The $T_>$ component is split in a few states centered at around 10 MeV excitation energy. The splitting of the strength of the $g_{9/2}$ state was already observed in Ref. [20] and it is probably increased in our case by the coupling to the $f_{7/2}$ hole state.

At higher excitation energies several small structures can be seen in the spectrum but no pronounced bump is observed. As in the case of the neutron stripping reactions, the proton stripping spectrum is dominated by a large continuum.

C. Pickup reactions

Figure 5 shows energy spectra measured for $^{209}\text{Bi}(^{20}\text{Ne}, ^{21}\text{Na})^{208}\text{Pb}$ at 48 MeV/nucleon, $^{209}\text{Bi}(^{36}\text{Ar}, ^{37}\text{K})^{208}\text{Pb}$, and $^{63}\text{Cu}(^{36}\text{Ar}, ^{37}\text{K})^{62}\text{Ni}$ at 42 MeV/nucleon. In the case of pickup reactions, the background at high excitation energy is low compared to the stripping reactions due to the absence of the projectile breakup contribution. A characteristic feature of all pickup spectra is also a rapid decrease of the cross section as a function of excitation energy. This can be understood since, as soon as the projectilelike nucleus is excited above its particle emission threshold, it will decay by particle emission and consequently will populate the inelastic channel. Only reactions in which the projectilelike nucleus is excited below its particle emission threshold will be observed in the spectra.

In the case of the proton pickup reactions on ^{209}Bi , the ground state, which is clearly visible in the spectra [Figs. 5(a) and 5(b)], corresponds to the pickup of the outmost proton from the $1h_{9/2}$ orbital outside the closed $Z=82$ proton shell. The collective 3^- state at 2.614 MeV, which has been reported in the $^{209}\text{Bi}(d, ^3\text{He})^{208}\text{Pb}$ reaction [21], is not observed in the present experiment. The spectra are dominated by a large peak centered at 5.5 MeV. In the energy range between 4 and 6 MeV, particle-hole states corresponding to $[1h_{9/2}, 3s_{1/2}^{-1}]$, $[1h_{9/2}, 2d_{3/2}^{-1}]$, $[1h_{9/2}, 2d_{5/2}^{-1}]$, and $[1h_{9/2}, 1h_{11/2}^{-1}]$ excitations have been reported [21,22], the two latter giving the largest contribution to the cross section. The present experimental resolution did not allow us to separate the high density of peaks identified in the cited $(d, ^3\text{He})$ experiments. In the $(^{20}\text{Ne}, ^{21}\text{Na})$ reaction, the contribution of the ejectile ground state ($2d_{3/2}$) is expected to be negligible compared to the first excited state, i.e., the 0.338 MeV $2d_{5/2}$ state [23]. For the $(^{36}\text{Ar}, ^{37}\text{Kr})$ experiment, mutual excitations with the first doublet state of ^{37}Kr ($f_{7/2}$) have to be added to the ground-state contribution. The energy difference between this state and the ground state (1.37 MeV) is comparable with the energy resolution. However, the high density of ^{208}Pb states does not allow one to distinguish between the different contributions of projectile states. The slight broadening of the 5.5 MeV peak in the ^{36}Ar reaction is probably an effect of the mutual excitation. At around 8

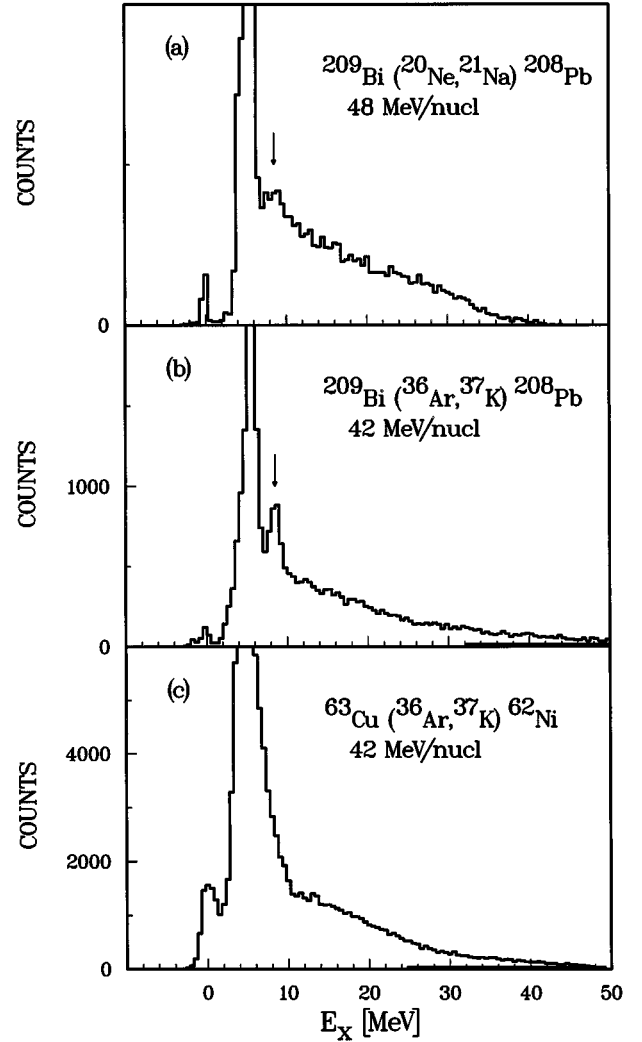


FIG. 5. Energy spectra measured for the ^{209}Bi target nucleus in the $(^{20}\text{Ne}, ^{21}\text{Na})$ (a) and $(^{36}\text{Ar}, ^{37}\text{K})$ (b) proton pickup reactions and for the ^{63}Cu target nucleus in the $(^{36}\text{Ar}, ^{37}\text{K})$ reaction (c).

MeV, a third peak is observed. A similar peak was also evidenced in the $^{209}\text{Bi}(^{12}\text{C}, ^{13}\text{N})^{208}\text{Pb}$ reaction [4]. This peak could be due to proton pickup from the $2d_{5/2}$ orbital. The peak is much more pronounced with the ^{36}Ar than with the ^{20}Ne and ^{12}C projectiles which can be well explained by the $j_<$ selectivity of ^{37}Kr . According to the energy and the selectivity, the 8 MeV state is likely to be dominated by $[1h_{9/2}, 2g_{7/2}]$ excitation.

The measured proton pickup spectra leading to the ^{208}Pb final nucleus have no similarity with the neutron stripping spectrum measured for the reaction $^{207}\text{Pb}(^{20}\text{Ne}, ^{19}\text{Ne})^{208}\text{Pb}$ leading to the same final nucleus. This suggests that no overlap exists between $[(njl), (3p_{1/2}^{-1})]$ particle-hole states excited in the stripping reaction and $[1h_{9/2}, (njl)^{-1}]$ states excited in the pickup reaction. In particular, no structure is observed at around 13 MeV in the pickup spectrum in contrast to the corresponding stripping reaction.

In the case of the proton pickup spectrum measured for the ^{63}Cu target [Fig. 5(c)], the ground state corresponds to the pickup of the proton from the $2p_{1/2}$ orbital. Above the

ground state, a peak having a width of about 4 MeV and centered at about 6 MeV excitation energy is observed in the spectrum. The width of this structure does not allow us to identify the eventual excitation of the projectile. In this excitation energy region, states corresponding to pickup from $2s_{1/2}$ and $1f_{7/2}$ proton orbitals have been reported [24], the latter being more favored by the projectile matching conditions. As in the case of the ^{209}Bi target nucleus, no giant-resonance-like structures are observed in the spectrum.

IV. RPA-DWBA CALCULATION

In order to estimate the cross section due to collective particle-hole excitations in stripping reactions, microscopic calculations were performed for the $^{207}\text{Pb}(^{20}\text{Ne},^{19}\text{Ne})^{208}\text{Pb}$ and $^{59}\text{Co}(^{20}\text{Ne},^{19}\text{F})^{60}\text{Ni}$ reactions. Collective excitations such as giant resonances are described in the random phase approximation (RPA) as a coherent sum of particle-hole excitations. When a particle is transferred to a target nucleus having a hole such as ^{207}Pb or ^{59}Co , a part of the particle-hole configurations contributing to the giant resonance strength can be excited. The strength of the collective excitations depends on the number of particle-hole configurations that can be excited in the transfer reaction and on the probability to transfer a nucleon to the corresponding particle states. In the case of the ^{207}Pb target, only two different particle states can be coupled to the $3p_{1/2}$ hole state for a given total angular momentum which makes it an unfavorable candidate for collective excitations. The relatively high spin of the $1f_{7/2}$ hole state in ^{59}Co allows a wider range of multiplicities and thus enhances the possibility of exciting collective strength. The transfer cross section including collective excitations can be estimated by

$$\frac{d\sigma}{d\Omega dE} = \sum_{\nu} \left| \sum_p A_p(E, \theta) X_{ph_0}^{\nu} \right|^2 \delta(E - E_{\nu}),$$

where A_p is the amplitude corresponding to the nucleon transfer to a given particle state during a scattering to an angle θ with an energy loss E . $X_{ph_0}^{\nu}$ is the RPA amplitude of a given particle-hole configuration ph_0 in an excited state ν . All bound and quasibound particle states were included in the calculation and different transitions to electric multipoles from $L=0$ to $L=9$ were considered. The transfer amplitude $A_p(E, \theta)$ was calculated by the code PTOLEMY by using the RPA wave functions to describe final states in the quasitarget nucleus. The cross section corresponding to three final states $2s_{1/2}$, $1p_{1/2}$, and $1d_{5/2}$ of ^{19}Ne and ^{19}F was summed with respective weights C^2S given by the spectroscopic factors of Ref. [15]. The collectivity of a given excited state is defined according to the number of particle-hole configurations in this state. In the case of ^{208}Pb , a state is defined to be collective if at least five particle-hole configurations contribute to the state, each with a relative weight less than 0.85. For ^{60}Ni , the equivalent definition used is at least three configurations with relative weight less than 0.9. These criteria were defined by requiring that the well-known giant resonances excited in inelastic scattering be collective states. A more detailed description of the calculation can be found in Refs. [17,25].

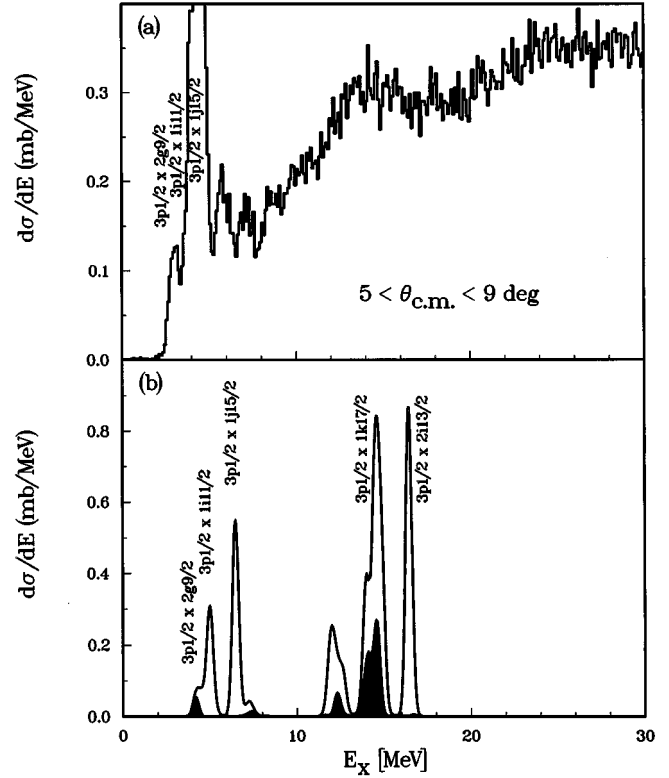


FIG. 6. Differential transfer cross section for the $^{207}\text{Pb}(^{20}\text{Ne},^{19}\text{Ne})^{208}\text{Pb}$ reaction. The upper part (a) presents the experimental and the lower part (b) the calculated transfer cross section. The collective strength is represented by the black area. The cross sections are integrated over the experimental angular domain.

In Fig. 6, the spectrum calculated for the neutron stripping reaction on ^{207}Pb is compared to the measured spectrum. It is important to note that neither damping nor continuum are included in the calculation. Therefore we cannot hope to reproduce the details of the experimental spectrum by the calculation. The low-lying states are rather well described although a shift of 1–2 MeV towards higher excitation energies is observed, which is a well-known property of RPA calculations. Moreover, the absolute cross section is comparable to the experimental one. At higher excitation energies, the calculation gives a strong concentration of the cross section between 12 and 17 MeV corresponding to the bump in the experimental spectrum. This is due to the excitation of high multiplicities ($L > 6$) corresponding to the following particle-hole configurations: $[k_{17/2}, p_{1/2}^{-1}]$, $[i_{13/2}, p_{1/2}^{-1}]$, $[j_{13/2}, p_{1/2}^{-1}]$, and $[h_{11/2}, p_{1/2}^{-1}]$. This is in qualitative agreement with the spin and parity assignment obtained by the angular distribution analysis. An important amount of collective strength, represented by the black shaded area, is observed at about 14 MeV but the single-particle strength clearly dominates the spectrum.

Figure 7 shows the calculated and measured proton stripping spectrum for the ^{59}Co target. The calculation predicts a very strong excitation of the $[f_{5/2}, f_{7/2}^{-1}]$ and $[g_{9/2}, f_{7/2}^{-1}]$ states while the ground state and the $[p_{3/2}, f_{7/2}^{-1}]$ state are not ex-

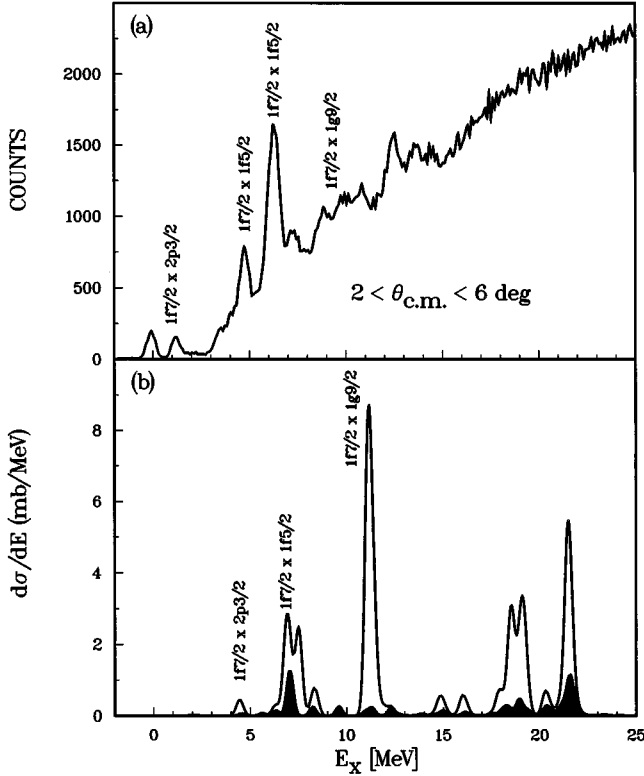


FIG. 7. Same as Fig. 6 for the $^{59}\text{Co}(^{20}\text{Ne}, ^{19}\text{F})^{60}\text{Ni}$ reaction.

cited. This is in agreement with the experimental observations discussed in Sec. III, except that the splitting of the $[g_{9/2}, f_{7/2}^-]$ peak observed experimentally is not reproduced by the calculation which does not include the coupling of states to the continuum.

Between 17 and 22 MeV two rather fragmented peaks are observed in the calculated spectrum. In this excitation energy region the largest cross section is due to multipoles $L > 5$ corresponding to $[h_{11/2}, f_{7/2}^-]$, $[f_{7/2}, f_{7/2}^-]$, and $[g_{7/2}, f_{7/2}^-]$ configurations, but no concentration of cross section is observed experimentally in this region. As in the case of the ^{207}Pb target, a small amount of collective strength is predicted by the calculation. In the case of ^{60}Ni , the agreement with the experimental spectrum is poorer than in the case of ^{208}Pb . This can be explained partly by the fact that the damping of states is not taken into account in the calculation. This could also indicate that the ^{60}Ni spectrum cannot be completely described without taking into account the coupling with the neutrons above the $N=28$ core.

As discussed in Ref. [17], collective excitations are predicted for low multipole modes while particle-hole correlations disappear for high multipoles. The matching conditions in the studied reactions favor the transfer to high angular momentum orbitals. In the case of ^{208}Pb this leads to favorable excitation of high multipole modes. In the case of ^{60}Ni , also low multipole modes can be reached but with a low cross section due to the spin factor $2J_B + 1$. For these reasons, the cross section for collective states is weak for both reactions.

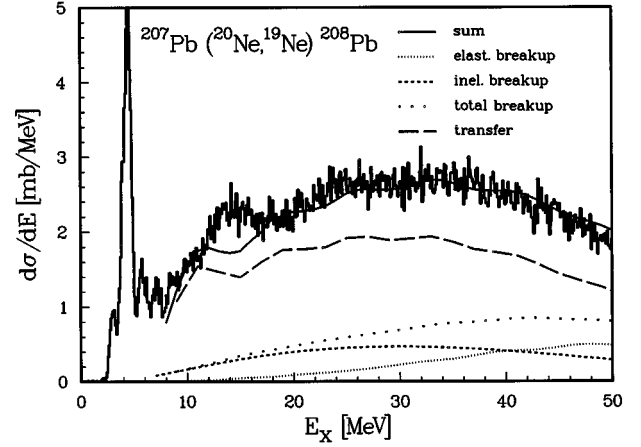


FIG. 8. Energy spectrum measured for the $^{207}\text{Pb}(^{20}\text{Ne}, ^{19}\text{Ne})^{208}\text{Pb}$ reaction at 48 MeV/nucleon. The total transfer cross section calculated by the Bonaccorso-Brink model is indicated by the solid line. Different contributions in the calculated spectrum are indicated as follows: (1) transfer to quasibound and unbound target states, (2) sum of the elastic and inelastic breakup processes, (3) elastic breakup processes, and (4) inelastic breakup processes.

V. SEMICLASSICAL CALCULATIONS

In stripping reactions between heavy ions at incident energies per nucleon higher than the average binding energy, a large part of the cross section is due to the nucleon transfer to unbound target states giving rise to a continuous spectrum. The Bonaccorso-Brink model [7,8] gives a description of the neutron transfer reactions to the quasibound and unbound target states. It also allows the estimation of the contribution of the projectile breakup processes to the inclusive stripping spectra. In this section we will compare the spectra measured for the $^{207}\text{Pb}(^{20}\text{Ne}, ^{19}\text{Ne})^{208}\text{Pb}$ and $^{207}\text{Pb}(^{36}\text{Ar}, ^{35}\text{Ar})^{208}\text{Pb}$ reactions to the spectra calculated by using the Bonaccorso-Brink model. Only the basic formalism and results are given, since a more detailed description of the calculation can be found in Refs. [25,26].

According to Bonaccorso and Brink, the transfer probability from an initial bound state of energy ε_i and angular momentum j_i to a final continuum state of ε_f and j_f is given by [7]

$$\frac{dP}{d\varepsilon_f}(j_f, j_i) = \sum_{j_f} [1 - \langle S_{j_f} \rangle]^2 + (1 - |\langle S_{j_f} \rangle|^2) B(j_f, j_i),$$

where $\langle S_{j_f} \rangle$ is the optical model S matrix which describes the rescattering of the neutron on the target and $B(j_f, j_i)$ is an elementary transfer probability. The term proportional to $|1 - \langle S_{j_f} \rangle|^2$ gives the elastic breakup contribution while the second term proportional to $1 - |\langle S_{j_f} \rangle|^2$ gives the absorption spectrum. In the elastic breakup processes the transferred nucleon is rescattered elastically from the target. The absorption cross section corresponds to transfer to the quasibound and unbound states in the target nucleus and to inelastic breakup reactions where the transferred nucleon rescatters inelastically leaving the target nucleus in an excited state.

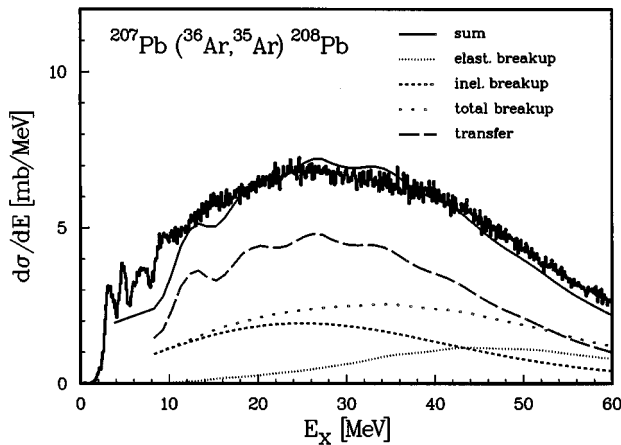


FIG. 9. Same as Fig. 8 for the $^{207}\text{Pb}(^{36}\text{Ar}, ^{35}\text{Ar})^{208}\text{Pb}$ reaction at 42 MeV/nucleon.

The inelastic breakup contribution can be estimated by calculating the absorption in the Born approximation [8].

The contributions of the first three ejectile hole states were considered in the calculation weighted by the corresponding spectroscopic factors. In the case of the ^{19}Ne ejectile the first hole states are $2s_{1/2}$, $1p_{1/2}$, and $1d_{5/2}$ and in the case of ^{35}Ar $1d_{3/2}$, $2s_{1/2}$, and $2p_{3/2}$. The spectroscopic factors were taken from Refs. [15] and [19], respectively. The optical potential used in the S -matrix calculation was that proposed by Mahaux and Sartor [27] for nucleon- ^{208}Pb . The influence of the different optical model parameters is studied in Ref. [25].

Figures 8 and 9 show the angle-integrated spectra measured for the $^{207}\text{Pb}(^{20}\text{Ne}, ^{19}\text{Ne})^{208}\text{Pb}$ and $^{207}\text{Pb}(^{36}\text{Ar}, ^{35}\text{Ar})^{208}\text{Pb}$ reactions, respectively. The dashed line represents the calculated total transfer cross section. The Bonaccorso-Brink model for the transfer to the continuum treats only quasibound and unbound states of the target nucleus and therefore the calculated spectra start only at the excitation energy corresponding to the binding energy of the neutron in the residual nucleus. In order to fit the experimental spectrum, the calculation has been normalized by a factor of 0.6 in the case of the the Ne projectile and by a factor of 0.1 in the case of the Ar projectile. In the limits of the experimental error bars and the theoretical uncertainties, the agreement between experimental and calculated transfer cross sections is relatively good in the case of Ne projectile but for the Ar projectile the calculation largely overestimates the total cross section.

The bumps that can be seen in the calculated spectra correspond to the transfer to the target resonance states. In the case of the $^{207}\text{Pb}(^{20}\text{Ne}, ^{19}\text{Ne})^{208}\text{Pb}$ reaction, the first structure at about 10 MeV is mainly due to the excitation of the $1k_{17/2}$ single-particle resonance state in ^{208}Pb . Even though this bump is located 3 MeV below the experimental one, its spin assignment corresponds to the bump seen in the experimental spectrum at 13.5 MeV and in the spectrum resulting from the microscopic calculation discussed in Sec. IV. This is in agreement with the interpretation of Refs. [2,10]. At higher excitation energies the calculation shows several weak structures which, however, remain inside the statistical

fluctuations of the experimental spectrum. The discrepancy between the position of the bump in the experimental and the theoretical spectra can be explained by the fact that in the BB model it is the overall description of the neutron + target optical model which determines the energy of the single-particle resonances.

The main purpose of this comparison was to ascertain if this model can reproduce the overall shape of spectra and give a reliable estimation of the breakup contribution. If the very high energy part (>50 MeV) of the spectrum is not considered, because it is outside the SPEG acceptance, the overall shape of the spectrum is well reproduced by the calculation. In the case of the $^{207}\text{Pb}(^{36}\text{Ar}, ^{35}\text{Ar})^{208}\text{Pb}$ reaction, the calculation as well as the experimental spectrum shows fewer structures than with the ^{20}Ne projectile. The overall shape of the spectrum is again well reproduced.

The different contributions due to the transfer to the target resonances states and the elastic and inelastic breakup processes are also indicated in Figs. 8 and 9. The elastic breakup spectrum is approximately centered at the incident energy per nucleon while the major contribution from the inelastic breakup processes is at lower apparent excitation energies. When the incident energy increases, the maximum of the total breakup spectrum moves towards higher apparent excitation energies, slightly changing the shape of the spectrum measured for neon projectiles at 48 MeV/nucleon compared to that measured with argon projectiles at 42 MeV/nucleon. It is interesting to notice that for these two reactions, the transfer to single-particle resonance states is still dominant, the cross section due to breakup processes being only about one-third of the total cross section. Experimentally the measurement of coincident neutrons would allow us to distinguish between breakup and transfer to resonant states. Such an experiment has been performed recently [28].

VI. CONCLUSION

Several one-nucleon transfer reactions were studied in the region of Pb and Ni by using Ne and Ar beams at 48 and 42 MeV/nucleon, respectively. Pronounced bumps superimposed on a large continuum are observed in several stripping spectra. In the Pb region, a bump is located at a Q value of -23 MeV while its excitation energy varies from 10 to 13 MeV depending on the target. This suggests that the structures are due to single-particle excitations. No structures were observed at excitation energies above 10 MeV in the measured pickup spectra.

The single-particle nature of the structures in the stripping spectra of ^{207}Pb and ^{59}Co is in agreement with a microscopic calculation where collective excitations are treated in the framework of the random phase approximation. In the studied reactions, the angular momentum matching condition favors the excitation of high multipole modes while collective effects are only seen in the case of low multipole modes.

The overall shape of the measured stripping spectra are fairly well reproduced by the Bonaccorso-Brink calculation. This model also allows us to estimate the projectile breakup contribution to the inclusive transfer spectra which is predicted to be about one-third of the total cross section.

- [1] Ph. Chomaz *et al.*, Annual Report, IPN-Orsay, 1990.
- [2] S. Fortier, S. Galès, Sam M. Austin, W. Benenson, G. M. Crawley, C. Djalali, J. S. Winfield, and G. Yoo, *Phys. Rev. C* **41**, 2689 (1990).
- [3] S. Galès, Ch. Stoyanov, and A. I. Vdovin, *Phys. Rep.* **166**, 125 (1988).
- [4] G. H. Yoo, G. M. Crawley, N. Orr, J. S. Winfield, J. E. Finck, S. Galès, Ph. Chomaz, I. Lhenry, and T. Suomijärvi, *Phys. Rev. C* **47**, 1200 (1993).
- [5] *Nucl. Data Sheets* **47**, 840 (1986).
- [6] *Nucl. Data Sheets* **48**, 340 (1986).
- [7] A. Bonaccorso and D. Brink, *Phys. Rev. C* **44**, 1559 (1991).
- [8] A. Bonaccorso and D. Brink, *Phys. Rev. C* **46**, 700 (1992).
- [9] L. Bianchi, B. Fernandez, J. Gastebois, A. Gillibert, W. Mittig, and J. Barrette, *Nucl. Instrum. Methods A* **276**, 509 (1989).
- [10] C. P. Massolo, F. Azaiez, S. Galès, S. Fortier, E. Gerlic, J. Guillot, E. Hourani, and J. M. Maison, *Phys. Rev. C* **86**, 1256 (1986).
- [11] M. C. Mermaz *et al.*, *Phys. Rev. C* **37**, 1942 (1988).
- [12] W. von Oertzen, *Phys. Lett.* **151B**, 95 (1985).
- [13] M. C. Mermaz *et al.*, *Z. Phys. A* **326**, 353 (1987); **327**, 207 (1987).
- [14] W. von Oertzen *et al.*, *Nucl. Phys.* **A487**, 195 (1988).
- [15] T. Engeland and P. J. Ellis, *Nucl. Phys.* **A181**, 700 (1972).
- [16] M. H. Macfarlane and S. C. Pieper, ANL Report No. ANL-76-11 (1976).
- [17] I. Lhenry, T. Suomijärvi, Ph. Chomaz, and Nguyen van Giai, *Nucl. Phys.* **A565**, 524 (1993).
- [18] D. Beaumel *et al.*, *Phys. Rev. C* **49**, 2444 (1994).
- [19] R. R. Johnson and R. J. Griffiths, *Nucl. Phys.* **A108**, 113 (1968).
- [20] M. Braeunig *et al.*, *Nucl. Phys.* **A519**, 631 (1990).
- [21] E. A. McClatchie, C. Glashauser, and D. L. Hendrie, *Phys. Rev. C* **1**, 1828 (1970).
- [22] G. Mairle *et al.*, *Phys. Lett.* **121B**, 307 (1983).
- [23] M. B. Burbank, G. G. Frank, N. E. Davidson, G. C. Neilson, S. S. M. Wong, and W. J. McDonald, *Nucl. Phys.* **A119**, 184 (1968).
- [24] G. Mairle, G. Th. Kaschl, H. Mackh, U. Schmidt-Roth, and G. J. Wagner, *Nucl. Phys.* **A134**, 180 (1969).
- [25] I. Lhenry, Ph.D. thesis, Report No. IPNO-T-92-01, Orsay, 1992.
- [26] A. Bonaccorso, I. Lhenry, and T. Suomijärvi, *Phys. Rev. C* **49**, 329 (1994).
- [27] C. Mahaux and R. Sartor, *Nucl. Phys.* **A493**, 157 (1989).
- [28] H. Laurent *et al.*, *Phys. Rev. C* **52**, 3066 (1995).